International Journal of Mass Spectrometry 296 (2010) 53–58

Contents lists available at ScienceDirect

International Journal of Mass Spectrometry

journal homepage: www.elsevier.com/locate/ijms

Production and utilization of CO_3^- produced by a corona discharge in air for atmospheric pressure chemical ionization

Robert G. Ewing[a,*], Melanie J. Waltman[a,b]

[a] Pacific Northwest National Laboratory, Richland, WA 99354, USA
[b] New Mexico Tech, Socorro, NM 87801, USA

ARTICLE INFO

Article history:
Received 28 June 2010
Received in revised form 27 August 2010
Accepted 27 August 2010
Available online 9 September 2010

Keywords:
APCI
IMS
CO_3^-
Corona discharge
Explosives

ABSTRACT

Atmospheric pressure chemical ionization is a multistep ionization process used in mass spectrometry and ion mobility spectrometry. The formation of product ions depends upon interactions with the analyte and the reactant ion species formed in the ionization source. The predominant reactant ion observed in a point-to-plane corona discharge in air occurs at m/z 60. There have been multiple references in the literature to the identity of this ion with some disagreement. It was postulated to be either CO_3^- or $N_2O_2^-$. The identity of this ion is important as it is a key to the ionization of analytes. It was determined here to be CO_3^- through the use of ^{18}O labeled oxygen. Further confirmation was provided through MS/MS studies. The ionization of nitroglycerine (NG) with CO_3^- produced the adduct $NG{\cdot}CO_3^-$. This was compared to ionization with NO_3^- and Cl^- reactant ions that also formed adducts with NG. The fragmentation patterns of these three adducts provides insight into the charge distribution and indicates that CO_3^- has a relatively high electron affinity similar to that of nitrate.

© 2010 Published by Elsevier B.V.

1. Introduction

Ion mobility spectrometry (IMS) is routinely used for the detection of explosives, drugs and chemical weapons in the field. The most common atmospheric pressure chemical ionization (APCI) source used in commercial IMS instruments is ^{63}Ni, a radioactive isotope [1]. The use of a radioactive isotope as an ionization source has many advantages, such as long term stability without requiring an additional power supply. Further, the ionization processes occurring with a ^{63}Ni source have been well investigated, and the subsequent product ions created are the basis for compound identification algorithms. Although radioactive ionization sources are reliable and well understood, the handling, accountability and potential for spreading radioactive contamination make ownership of these devices cumbersome and costly. The requirement to maintain control of the source prohibits the use of such instruments where nonrecoverable loss, such as inserting the instrument into bore holes or flying in unmanned aircraft, could occur. Due to these and many other concerns in handling radioactive isotopes, there is a desire to find a suitable nonradioactive ionization source with similar ionization properties to those of ^{63}Ni.

There are a variety of APCI sources, such as corona discharge ionization, photoionization, laser ionization and flame ionization. Of these, corona discharge appears to produce positive ions similar to those from ^{63}Ni [2] and contains operational characteristics that meet the requirements of a hand-portable device. Corona discharge sources have been investigated for use in a handheld IMS [3], and this has been developed into the commercial device LCD 3.3 (Smiths Detection, Watford, UK).

The negative reactant ions created were different than $O_2^-{\cdot}(H_2O)_n$ ions generated with ^{63}Ni sources, a challenge in the development of corona discharge for IMS. Corona discharge sources typically produce nitrite and nitrate ions with limited reactivity due to their inherently high electron affinities [4]. One of the goals in the development of IMS systems with corona discharge ionization sources was to produce reactant ions similar to those generated with a ^{63}Ni source, mainly O_2^- ions. To achieve this, a pulsed corona was explored [4] as was adding a counter-current flow to the source region [5]. Ozone and NO_x generated in the discharge lead to the production of nitrite and nitrate ions. Using a short pulse of the corona discharge or providing a counter-current flow of gas resulted in a decrease in the amount of neutral ozone or NO_x, which enabled O_2^- reactant ions to persist in the reaction region. In addition to the nitrite and nitrate ions, corona discharge sources have also been shown to produce O_2^-, O_3^- and an anion at m/z 60 along with hydrates of these ions [6,7].

We have observed in APCI-MS studies that the negative ion at m/z 60 is the predominant ion generated in air with a point-to-plane corona discharge under normal operating conditions and gas flows. A molecular weight of 60 amu could occur with an ion containing

---

* Corresponding author. Tel.: +1 509 375 6453.
E-mail address: Robert.ewing@pnl.gov (R.G. Ewing).

1387-3806/$ – see front matter © 2010 Published by Elsevier B.V.
doi:10.1016/j.ijms.2010.08.024

Table 1
Electron affinities of typical reactant ions observed at API conditions. Ranges collected from the NIST Webbook [14].

Species	Electron affinity
Cl	3.6 eV
O_2	0.40–1.3 eV
O_3	1.8–2.5 eV
NO_2	1.8–3.9 eV
NO_3	3.7–3.9 eV
CO_3	1.8–3.5 eV

either one carbon and three oxygen atoms or two nitrogen and two oxygen atoms. With the limits of resolution in a quadrupole system, it is impossible to tell the difference between CO_3^- and $N_2O_2^-$. There is some uncertainty in the literature whether CO_3^-, or $N_2O_2^-$ is the ion formed at *m*/*z* 60 at atmospheric pressure with a corona discharge. Many studies have indicated the formation of CO_3^- with mechanisms for the formation involving O_3^- and CO_2, although many of these were performed at subambient pressures (5–27 kPa) [6]. Other studies have shown the generation of $N_2O_2^-$ anion by an electron beam ionized free jet expansion or pulsed supersonic discharge source with O_2 and N_2, pure N_2O, and NO and argon [8,9]. Through pulsed photoelectron spectroscopy three distinguishable forms of $N_2O_2^-$ were observed including $O_2^-{\cdot}N_2$, $O^-{\cdot}N_2O$, or $NO^-{\cdot}NO$. This was noted by Donò et al. while looking at the abatement of volatile organic compounds by corona discharge [10]. Donò et al. noted the dilemma in ion identity mentioned above, and they favored $(NO)_2^-$ since NO is a known product of discharges in air. Further, studies of corona discharges have discussed the production N_2O along with ozone [11] lending to the possibility of the formation of either CO_3^- or $N_2O_2^-$. Siegel noted the presence of the *m*/*z* 60 with a ^{63}Ni ionization source and recognized that it could have been CO_3^- but believed it was an adduct of O_2^- with N_2 [12].

A recent publication by Sabo et al. investigated the identity of the *m*/*z* 60 ion by IMS and MS from a corona discharge in high purity oxygen [13]. They suggested the ion was $N_2O_2^-$ based upon the discharge occurring in high purity oxygen with sub-ppb levels of water and carbon dioxide. They attributed the formation of this ion to the trace (ppm) levels of nitrogen in their oxygen forming N_2O with subsequent reactions of N_2O with either O^- or O_3^- producing $N_2O_2^-$.

Since the ionization of explosives, pesticides, blister agents and other chemicals relies on negative atmospheric pressure chemical ionization, the identity of the negative reactant ions available will affect subsequent product ion formation. Changes to the reactant ions will affect the ionization mechanisms of analytes. Such mechanisms include charge transfer, proton abstraction or adduct formation, and changes to the reactant ion can lead to changes in sensitivity or product ion identity. For example, if the ionization mechanism is charge transfer, relative electron affinities between the reactant ion and the analyte will determine the potential for ionization to occur. The ranges of electron affinities for potential negative reactant ions are provided in Table 1. Since IMS relies on mobility as the means for identification, changes to ion identity will change the mobility and require subsequent alterations to detection algorithms. The need to better understand the ionization chemistry that occurs in IMS and APCI-MS using corona discharge sources, motivated this effort to identify the ion at *m*/*z* 60.

2. Experimental

2.1. Chemicals and gases

Ultrahigh purity (UHP) nitrogen, UHP argon and oxygen were obtained from Matheson Tri-Gas, (Albuquerque, NM). ^{18}O labeled oxygen, 95% purity, was obtained from Cambridge Isotope Laboratories, Inc. (Andover, MA). Nitroglycerine (NG) standard was obtained from Cerilliant Corp. (Round Rock, TX) at 1000 μg/mL in acetonitrile, and working solutions were diluted in methanol to 1:10 for concentrations of 100 ng/μL. Carbon tetrachloride was from Thermo Fisher Scientific Inc. (Waltham, MA).

2.2. Instrumentation

The atmospheric pressure ionization triple quadrupole mass spectrometer used in these studies was an API-III (AB SCIEX, Rexdale, Ontario). Data were collected on a Macintosh Quadra 400 using API-Tune software provided with the instrument. It was operated with the factory heated nebulizer probe and a corona discharge ionization source. Typical interface voltages were between −300 and −600 VDC. The negative corona discharge current was set at 3 μA. The other lens voltages were as follows: Pinhole (OR) = −35, R0 = −30, R1 = −27, R2 = 45 and R3 = 70. For MS/MS operations, argon was used as the collision gas with a collision gas thickness of 125×10^{12} molecules cm^{-2}. The voltage measured between OR and R2, which determined the energy of the ion entering the collision cell, was 80 V. Nitrogen was used as the curtain gas with a flow of 400 mL/min that swept across the pinhole and out a hole in the interface plate counter current to ion movement. Nitrogen was used in the auxiliary, and oxygen in the nebulizer gas ports. Specific flows varied by experiment. Both the auxiliary and nebulizer gasses combined and flowed across the corona discharge needle and towards the pinhole of the mass spectrometer. The corona discharge was enclosed in a cylindrical chamber with the gasses vented out a port at the bottom of the chamber.

To obtain spectra generated with a ^{63}Ni ionization source, the corona needle was removed, and a cylindrical ^{63}Ni source housed within a Teflon block was placed at the end of the nebulizer probe. Sample flow from the heated nebulizer passed through the ^{63}Ni source toward the inlet of the mass spectrometer. The source was floated −400 VDC below the interface voltage so that anions would move from the ^{63}Ni source toward the mass spectrometer.

Solutions of 100 μL of MeOH containing 10 μg of NG were added to the glass liner of the heated nebulizer while at ambient temperature and no gas flow. After the solvent was allowed to evaporate, the nebulizer heater was turned on (set point of 150 °C) to desorb the explosive. At this time, the auxiliary and nebulizer flows were turned on at rates of 500 mL/min and 100 mL/min, respectively. Significant quantities of NG remained in the ionization region and were persistent in the spectra for approximately 10–20 min. Each spectrum collected was the result of approximately 25 scans (averaged).

3. Results and discussion

Representative mass spectra of ions generated at atmospheric pressure of mixtures of nitrogen and oxygen are displayed in Fig. 1. These spectra are essentially identical to similar spectra collected with purified air. Fig. 1A represents ions formed with a ^{63}Ni source, and Fig. 1B ions formed with a point-to-plane corona discharge ionization source. Predominant ions generated with ^{63}Ni include O_2^-, $O_2^-{\cdot}H_2O$ and $O_2^-{\cdot}CO_2$ at *m*/*z* of 32, 50 and 76 amu, respectively with gas flows of 2000 mL/min N_2 into auxiliary, 10 mL/min O_2 into nebulizer, and a curtain flow of 400 mL/min N_2. Typical ions generated with the point-to-plane corona discharge are O_2^-, O_3^- and the ion at *m*/*z* 60. The ion observed at *m*/*z* 60 is the largest ion, with O_3^- being only 15% and O_2^- only 5% of the intensity of this peak under conditions of discharge current (−3 μA), curtain flow of 400 mL/min of nitrogen, auxiliary flow of 400 mL/min of N_2 and nebulizer flow of 100 mL/min of O_2.

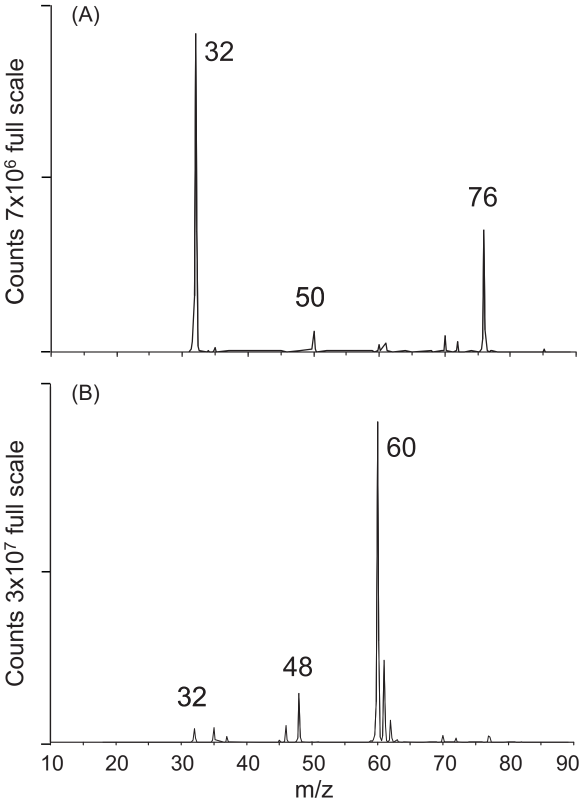

Fig. 1. Mass spectra of background ions generated in a mixture of nitrogen and oxygen with (A) a ^{63}Ni ionization source and (B) a corona discharge ionization source.

Corona discharge parameters, including discharge current and gas flow rates, were varied to observe the effects on the relative abundances of the ions formed. The ranges for conditions were as follows: discharge current was 1–5 μA; curtain gas was 300–2000 mL/min; and sample gas was 800–5600 mL/min, which was the sum of the auxiliary and nebulizer gasses. Ion intensities at masses of 32, 46, 48, 50, 60, 62, and 76 were monitored under the various conditions. In almost all cases, *m*/*z* 60 was the most prevalent ion. The relative intensities of the ions varied with changes to the flow and the discharge current. For example, with the sample gas fixed at 800 mL/min and the discharge set at 5 μA, a curtain gas flow of 300 mL/min produced ions at *m*/*z* 46, 48 and 62 that were similar in intensity to the 60 ion. However, as the curtain gas flow increased from 300 to 2000 mL/min, ions at *m*/*z* 48, 62 and 46 decreased relative to the 60 ion. This is likely due to the dilution of ozone and NO_x produced in the discharge with increased flows. Similar observations were noted by Ross and Bell [5]. The opposite behavior was noted upon increasing the discharge current while gas flows were held constant, yielding a subsequent increase in *m*/*z* 46, 48 and 62. Previous studies with a dielectric barrier discharge source showed that enclosing the source caused a shift in the predominant ion from *m*/*z* 60 to 62, indicating the formation the nitrate ion [15]. It was postulated that placing the source in an enclosure allowed concentrations of ozone and NOx to increase, which produced nitrate as the principal ion. However, in commercial APCI mass spectrometers using a point-to-plane corona discharge in clean air, the ion at *m*/*z* 60 appears to dominate the spectra.

Knowing the identity of the *m*/*z* 60 is important for understanding the subsequent ionization of analytes. One possible way of identifying the peak at *m*/*z* 60 would be to look at the isotopic abundances of C, N, and O at *m* + 1 and *m* + 2 to determine the number of carbon, nitrogen and oxygen atoms present. If the ion at *m*/*z* 60 was CO_3^-, then values (percent of the ion at *m*/*z* 60) of *m* + 1 = 1.19% and *m* + 2 = 0.62% would be expected. If the ion was $N_2O_2^-$ then values of *m* + 1 = 0.81% and *m* + 2 = 0.41% would be expected. Actual values of *m* + 1 and *m* + 2 were 25.63% and 6.89%, respectively, as shown in Fig. 1B, which are much higher percentages than those predicted from isotopic abundances alone. These values must result from contributions of other ionic species such as NO_3^- at *m*/*z* 62.

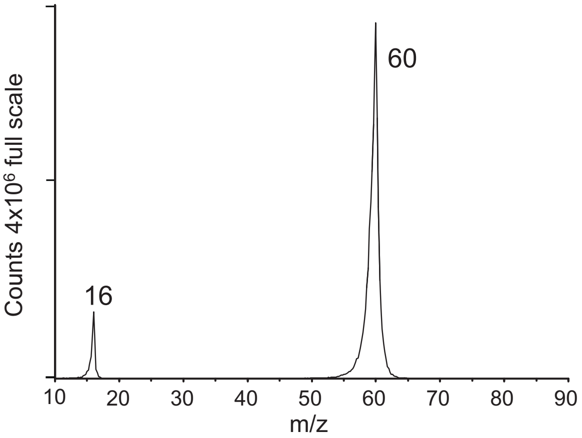

Fig. 2. MS/MS of the *m*/*z* 60 ion showing the only fragment ion at *m*/*z* 16 (O^-).

Fragmentation of the *m*/*z* 60 ion using MS/MS was another method attempted to elucidate its structure and composition. It was hoped that the daughter ions would give insight into the identity of the parent ion. As shown in Fig. 2, the only ion produced from the fragmentation of *m*/*z* 60 is the ion at *m*/*z* 16, O^-. Although this provided some information, it did not help in identifying the ion at *m*/*z* 60 since it is possible that this ion could be generated from the fragmentation of either CO_3^- or $N_2O_2^-$.

The ionization process to create either CO_3^- or $N_2O_2^-$ involves oxygen. The use of isotopically labeled oxygen could enable the identification of the *m*/*z* 60 ion. Upon using ^{18}O labeled oxygen, the ion at *m*/*z* 60 would shift two mass units for every ^{18}O atom present in the ion. Due to the cost of this gas and the high flow rates normally used in the APCI source, the flows were modified in an attempt to use as little oxygen as possible but to maintain the same observed ionization chemistry. The oxygen was removed from the nebulizer gas port and replaced with UHP nitrogen, and the source was purged with nitrogen (at a total flow rate of 2 L/min) while monitoring the mass spectra. After several minutes, the intensities of all ions began to decrease. The purge with nitrogen was allowed to continue until the ion signal had dissipated, showing only noise in the spectrum (4×10^4 counts compared to 5×10^7 counts for a typical spectrum). At this point, it was presumed that the majority of oxygen had been removed and only electrons were present. Oxygen was then metered into the ionization region through the nebulizer gas port. The level was slowly increased, and it was noted that significant ion signal was observed at a flow rate of 5 mL/min of oxygen. With an auxiliary flow rate of 2000 mL/min of nitrogen, the oxygen concentration was about 0.25%. The mass spectrum with these flow rates is shown in Fig. 3A and appeared similar to the ionization of air in a corona discharge. The ion at *m*/*z* 60 is the dominant ion present. This experiment was then repeated with $^{18}O_2$ in place of oxygen. With the addition of 5 mL/min of ^{18}O labeled oxygen, the peaks shifted from *m*/*z* 32, 48 and 60 to *m*/*z* 36, 54 and 62 corresponding to $^{18}O_2^-$, $^{18}O_3^-$ and $CO_2{}^{18}O^-$ as shown in Fig. 3B. The relative ion abundances resulting from both the labeled and unlabeled oxygen are essentially identical with the shifts in mass due to the labeled oxygen. From this data, it is presumed that *m*/*z* 60 is CO_3^-, where the ionization occurs with an ion and neutral CO_2, thus providing only one labeled oxygen atom. The formation of

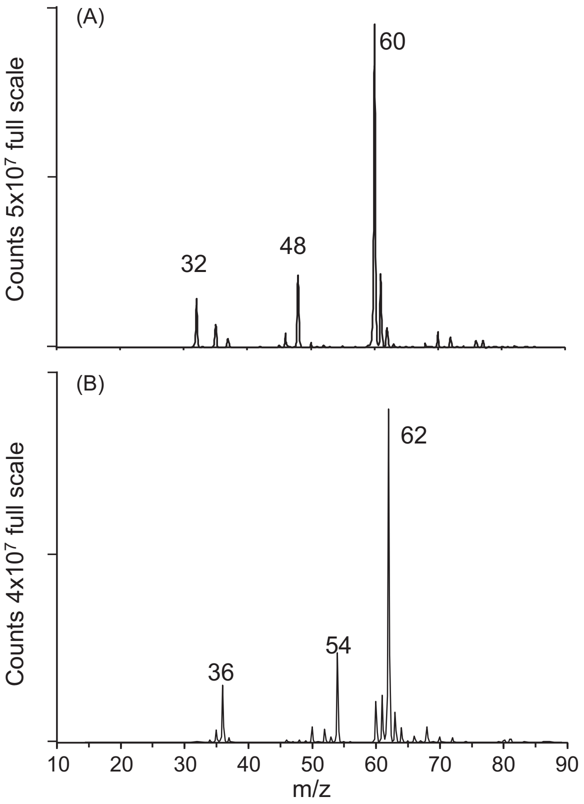

Fig. 3. Mass spectra of the corona discharge with N_2 and (A) 5 mL/min of $^{16}O_2$ oxygen and (B) 5 mL/min $^{18}O_2$ labeled oxygen.

CO_3^- likely comes from a reaction between O_3^- and CO_2 as a result of ozone, which is generated from $^{18}O_2$ in the electric discharge.

$$^{18}O_3^- + C^{16}O_2 \rightarrow C^{18}O^{16}O_2^- + {}^{18}O_2$$

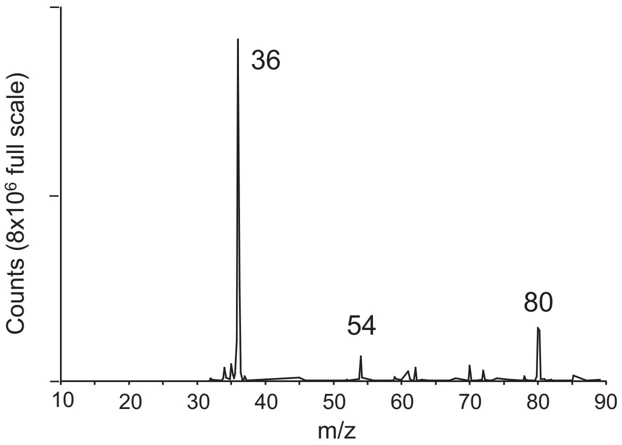

Fig. 4. Mass spectrum of ions generated with ^{63}Ni ion source and $^{18}O_2$ in nitrogen.

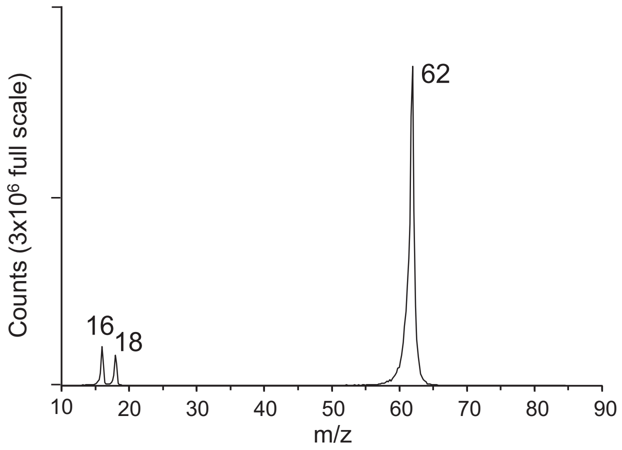

Fig. 5. MS/MS of the *m*/*z* 62 ion generated using $^{18}O_2$ labeled oxygen.

The corona needle was replaced by the ^{63}Ni source while maintaining the same flows using labeled oxygen. Fig. 4 shows the results of using ^{18}O labeled oxygen with the ^{63}Ni ionization source. As expected, the ions at *m*/*z* 32, 48 and 76 shifted to *m*/*z* 36, 54 and 80 corresponding to $^{18}O_2^-$, $^{18}O_3^-$ and $CO_2{}^{18}O_2^-$. The CO_2 is likely present as an impurity in the gas streams themselves or from small diffusion from the surrounding room air. The presence of CO_2, even in relatively pure gas streams, is expected at small levels (low ppm$_v$ range), similar to low ppm$_v$ amounts of water in zero air. Globally averaged concentration of CO_2 in air is around 383 ppm$_v$ [16] and is generally higher in urban areas. CO_2 in room air can be up to 10 times higher than background levels. For the reaction

$$O_3^- + CO_2 \rightarrow CO_3^- + O_2$$

with a rate constant $k = 5.5 \times 10^{-10}$ cm^3/s, and an assumed CO_2 concentration of 0.1 ppm (1.8×10^{12} cm^{-3}) [17] the reaction time is about 1 ms. At higher concentrations of CO_2, even faster reactions times would result. Thus, the presence of CO_2 is expected and is attributed to the formation of CO_3^-.

To confirm the ion identity of *m*/*z* 60 as CO_3^-, MS/MS fragmentation was performed on *m*/*z* 62 that was formed with the $^{18}O_2$ in the corona discharge. Fragment ions were produced at *m*/*z* 16 and 18 as shown in Fig. 5. The abundance of *m*/*z* 16 to 18 is approaching a 2:1 ratio, implying the identity as $C^{16}O_2{}^{18}O^-$. In contrast, fragmentation of NO_3^- (also *m*/*z* 62) produced different ions at *m*/*z* 32 and 46, which are O_2^- and NO_2^-. This indicates that the ion at *m*/*z* 62 formed in a corona discharge with $^{18}O_2$ is different than the nitrate ion formed at *m*/*z* 62 in a corona discharge in air. This fragmentation pattern can be compared to the fragmentation displayed in Fig. 2 of *m*/*z* 60, which shows only *m*/*z* 16 as a fragment. These fragmentation patterns along with the use of ^{18}O labeled oxygen confirmed the identity of the *m*/*z* 60 ion as CO_3^-.

To emphasize the importance of understanding the reactant ion chemistry and its role on product ion formation, the ionization of NG was explored with a variety of reactant ions including CO_3^-, Cl^- and NO_3^-. CO_3^- was produced with the corona discharge in air, chloride ions were formed by adding carbon tetrachloride to the corona source and nitrate ions were formed in an enclosed distributed plasma ion source described previously [15]. The ionization of NG with nitrate reactant ions formed from the distributed plasma ionization source formed an adduct between nitrate and NG as shown in Fig. 6A. The spectrum mostly contained NO_3^- at *m*/*z* 62 and NG·NO_3^- at *m*/*z* 289. With a point-to-plane corona where the main ion was CO_3^-, addition of NG provided a more complex spectrum displayed in Fig. 6B. In this spectrum, many ions are evident including: NO_2^-, CO_3^-, NO_3^- and adducts NG·CO_3^- and NG·NO_3^-. Although CO_3^- is the predominant reactant ion, O_2^- and O_3^- are also present and thought to interact with NG to produce the NO_2^- and NO_3^- observable in the spectrum. When NG was added in the presence of a chloride ion, the NG·Cl^- adduct was formed, as shown in Fig. 6C, at *m*/*z* 262 and 264. Nitrate and nitrite ions were also observed in the presence of the chloride reactant ion, and thought to result from complex ionization processes occurring in the discharge region.

Collision induced dissociation of the adducts of NO_3^-, CO_3^- and $^{35}Cl^-$ with NG were performed to investigate the fragment ions pro-

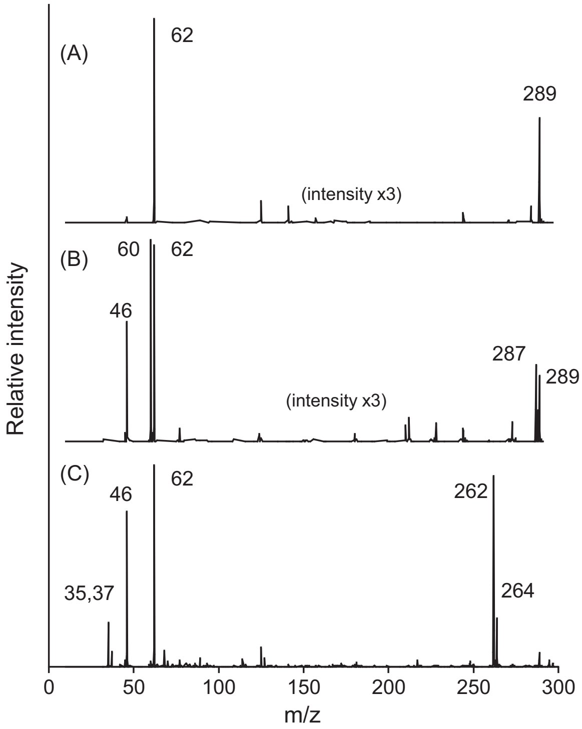

Fig. 6. Mass spectra of nitroglycerine (mw = 227) (A) from a distributed plasma ionization source, (B) from a corona discharge ionization source and (C) from a corona discharge with carbon tetrachloride.

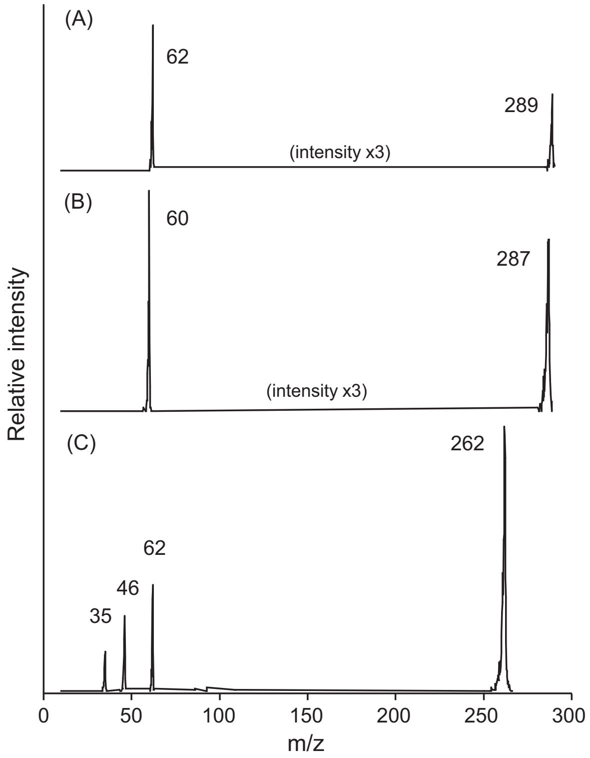

Fig. 7. MS/MS of nitroglycerine adducts (A) from a distributed plasma ionization source (*m*/*z* 289, NO_3^- adduct), (B) from a corona discharge ionization source (*m*/*z* 287, CO_3^- adduct) and (C) from a corona discharge with carbon tetrachloride (*m*/*z* 262, $^{35}Cl^-$ adduct).

duced. These MS/MS spectra are displayed in Fig. 7. Fragmentation of $NG{\cdot}CO_3^-$ yields *m*/*z* 60 (Fig. 7B) where fragmentation of $NG{\cdot}NO_3^-$ produces the NO_3^- ion (A). The fact that CO_3^- is the only fragment of the $NG{\cdot}CO_3^-$ adduct may indicate a high electron affinity of CO_3^-, ranking it close to that of NO_3^- (3.7–3.9 eV). In the NIST Webbook [14], electron affinity values for CO_3^- range from 1.8 to 3.5 eV with later references indicating higher values. The fragmentation pattern here indicates the charge resides with CO_3^- and tends to support the high values listed. It is noteworthy that under similar fragmentation conditions, the chloride adduct fragments into multiple ions: NO_3^-, NO_2^- and Cl^-, with NO_3^- being the largest fragment peak as shown in Fig. 7C. In IMS studies [18] it was shown that the chloride adduct of NG, when heated in an IMS above about 130 °C, fragments to only the nitrate ion. This was believed to be due to the high electron affinity of the nitrate (higher than that of chloride). However the fragmentation pattern shown here is different, possibly indicating a different mechanism. Essentially, in IMS studies, fragmentation occurs via thermal decomposition and here it is collisionally induced. This indicates that comparisons between the mass spectral data and the IMS data may not be directly correlated.

4. Conclusions

It was determined that the *m*/*z* 60 ion present as the most prevalent anion in a point-to-plane corona discharge source in air is CO_3^-. Further, it is likely generated by the reaction of O_3^- with CO_2. Since this is the predominant reactant ion available, it will affect the outcome of the ionization of analytes. For example, CO_3^- was shown to ionize NG by creating an adduct. Upon fragmentation of this adduct, CO_3^- is the only fragment seen. This points to a high electron affinity for CO_3^-, near that of NO_3^- and possibly higher than Cl^-. In other atmospheric pressure ionization sources such as ^{63}Ni, which is commonly used in commercial IMS instruments, different reactant ion species are formed. Thus, if corona discharge is a candidate for a nonradioactive ionization source, the reactant ion creation and subsequent analyte ionization needs to be explored to determine its efficacy as an ionization source.

References

[1] G.A. Eiceman, Z. Karpas, Ion Mobility Spectrometry, second ed., CRC Press, Boca Raton, Florida, 2005.
[2] L. Dzidic, D.I. Carroll, R.N. Stillwell, E.C. Horning, Atmospheric pressure ionization (API) mass spectrometry. Formation of phenoxide ions from chlorinated aromatic compounds, Anal. Chem. 47 (1976) 1308–1312.
[3] S.J. Taylor, L.J. Piper, J.A. Conner, J. FitzGerald, J.H. Adams, C.S. Harden, D.B. Shoff, D.M. Davis, R.G. Ewing, Design aspects and operation characteristics of the lightweight chemical detector, Int. J. Ion Mobility Spectrom. 1 (1998) 58–63.
[4] C.A. Hill, C.L.P. Thomas, A pulsed corona discharge switchable high resolution ion mobility spectrometer-mass spectrometer, The Analyst 128 (2003) 55–60.
[5] S.K. Ross, A.J. Bell, Reverse flow continuous corona discharge ionization applied to ion mobility spectrometry, Int. J. Mass Spectrom. 218 (2002) L1–L6.
[6] J.D. Skalny, T. Mikoviny, S. Matejcik, N.J. Mason, An analysis of mass spectrometric study of negative ions extracted from negative corona discharge in air, Int. J. Mass Spectrom. 233 (2004) 317–324.
[7] B. Gravendeel, F.J. de Hoog, Clustered negative ions in atmospheric negative corona discharges in the Trichel regime, J. Phys. B: At. Mol. Phys. 20 (1987) 6337–6361.
[8] D.L. Osborn, D.J. Leahy, D.R. Cyr, D.M. Neumark, Photodissociation spectroscopy and dynamics of the $N_2O^-{}_2$ anion, J. Chem. Phys. 104 (1996) 5026–5039.
[9] L.A. Posey, M.A. Johnson, Pulsed photoelectron spectroscopy of negative cluster ions: Isolation of three distinguishable forms of $N_2O^-{}_2$, J. Chem. Phys. 88 (1988) 5383–5395.
[10] A. Donò, C. Paradisi, G. Scorrano, Abatement of volatile organic compounds by corona discharge. A study of the reactivity of trichloroethylene under atmospheric pressure ionization conditions, Rapid Comm. Mass Spectrom. 11 (1997) 1687–1694.
[11] D.K. Brandvold, P. Martinez, The NO x. /N. 2. O fixation ration from electrical. discharges, Atm. Environment. 22 (1998) 477–480.
[12] M.S. Siegel, W.L. Fite, Terminal ions in weak atmospheric pressure plasmas. Applications of atmospheric pressure ionization to trace impurity analysis in gases, J. Phys. Chem. 80 (1976) 2871–2881.
[13] M. Sabo, J. Palenik, M. Kucera, H. Han, H. Wang, Y. Chu, S. Matejcik, Atmospheric pressure corona discharge ionization and ion mobility spectrometry/mass

spectrometry study of the negative corona discharge in high purity oxygen and oxygen/nitrogen mixtures, Int. J. Mass Spectrom. 293 (2010) 23–27.
[14] http://webbook.nist.gov/chemistry/form-ser.html accessed on June 7, 2010.
[15] M.J. Waltman, P. Dwivedi, H.H. Hill, W.C. Blanchard, R.G. Ewing, Characterization of a distributed plasma ionization source (DPIS) for ion mobility spectrometry and mass spectrometry, Talanta 77 (2008) 249–255.
[16] R.F. Keeling, S.C. Piper, A.F. Bollenbacher, J.S. Walker, Atmospheric Carbon Dioxide record from Mauna Loa, Carbon Dioxide Information Analysis Center, accessed at http://cdiac.ornl.gov/trends/co2/sio-mlo.html on June 3, 2010.
[17] M.T. Bowers (Ed.), Gas Phase Ion Chemistry, Vol. 1. Academic Press, New York, 1979.
[18] C.J. Miller, R.G. Ewing, Thermal Stability Study of Nitroglycerin and Structurally Related Chemicals, 55th ACS Northwest Regional Meeting (NORM), 2000.